Dynamics of kinks in one- and two-dimensional hyperbolic models with quasidiscrete nonlinearities

Horacio G. Rotstein,[1,*] Igor Mitkov,[2] Anatol M. Zhabotinsky,[1] and Irving R. Epstein[1]
[1]*Department of Chemistry and Volen Center for Complex Systems, Brandeis University, MS 015, Waltham, Massachusetts 02454-9110*
[2]*Department of Physics and CIRCS, Northeastern University, Boston, Massachusetts 02115*
(Received 6 November 2000; published 29 May 2001)

We study the evolution of fronts in the Klein-Gordon equation when the nonlinear term is inhomogeneous. Extending previous works on homogeneous nonlinear terms, we describe the derivation of an equation governing the front motion, which is strongly nonlinear, and, for the two-dimensional case, generalizes the damped Born-Infeld equation. We study the motion of one- and two-dimensional fronts finding a much richer dynamics than in the homogeneous system case, leading, in most cases, to the stabilization of one phase inside the other. For a one-dimensional front, the function describing the inhomogeneity of the nonlinear term acts as a ''potential function'' for the motion of the front, i.e., a front initially placed between two of its local maxima asymptotically approaches the intervening minimum. Two-dimensional fronts, with radial symmetry and without dissipation can either shrink to a point in finite time, grow unboundedly, or their radius can oscillate, depending on the initial conditions. When dissipation effects are present, the oscillations either decay spirally or not depending on the value of the damping dissipation parameter. For fronts with a more general shape, we present numerical simulations showing the same behavior.

DOI: 10.1103/PhysRevE.63.066613 PACS number(s): 45.05.+x, 46.05.+b, 63.20.Ry

I. INTRODUCTION

In the last few years, partial differential equations with discrete nonlinearities have been used to model phenomena in fields ranging from physics to biology, including the study of pinning of dislocation motions in crystals, breathers in nonlinear crystal lattices, Josephson junction arrays, and the biophysical description of calcium release waves [1–18]. Recently, the discrete one-dimensional stationary version of the Klein-Gordon equation

$$\phi_{tt}+\gamma\phi_t=D\phi_{xx}+\alpha\sum_k \delta(x-x_k)[f(\phi)+h], \qquad (1)$$

where $\gamma=0$ has been analyzed by Flach and Kladko [1] (see also references therein). In Eq. (1), ϕ is an order parameter, the non-negative constant γ is the dissipation coefficient, and the positive constants D and α are the diffusion coefficient and the amplitude of the discrete nonlinearity, respectively. The function f is a bistable function (the derivative of a double-well potential having two equal minima), i.e., a real odd function with positive maximum equal to ϕ^*, negative minimum equal to $-\phi^*$, and precisely three zeros in the closed interval $[a_-,a_+]$ located at a_-, a_0, and a_+. For simplicity and without lost of generality, we will consider in our analysis $a_-=-1$, $a_0=0$, and $a_+=1$. The prototype example is $f(\phi)=(\phi-\phi^3)/2$. The constant h, assumed to be small in absolute value, specifies the difference of the potential minima of the system, i.e., $f(\phi)+h$ is the derivative of a double-well potential with one local minimum and one global minimum. Note that Eq. (1) reduces to the Klein-Gordon equation when $\Sigma_k\delta(x-x_k)$ is replaced by a constant with appropriate rescaling. In Ref. [1] a first-order perturbation calculation for the heteroclinic orbits of the corresponding stationary kink solution for Eq. (1) was presented. Kink solutions, connecting the two local minima of the double-well potential, were also obtained for the sine-Gordon case $f(\phi)=-\sin(\phi)$, and the Klein-Gordon case $f(\phi)=(\phi-\phi^3)/2$. Both are particular cases of the function $f(\phi)$ as defined above. Note that the sine-Gordon case is equivalent to the derivative of a double-well potential in a restricted domain of definition.

In this paper, we study the dynamics of kinks for a quasidiscrete version of the Klein-Gordon equation

$$\phi_{tt}+\gamma\phi_t=D\Delta\phi+\alpha\beta(x,y)[f(\phi)+h] \qquad (2)$$

in a bounded region $\Omega\subset\mathbb{R}^n$, $n=1,2$ with smooth boundary $\partial\Omega$ for Neumann boundary conditions on $\partial\Omega$. When the function $\beta=\beta(x)$ is one-dimensional and $\beta(x)=\Sigma_k\delta(x-x_k)$, Eq. (2) reduces to Eq. (1). Although the analysis presented below will be valid for a general class of positive differentiable functions β, we have in mind some particular cases that approximate a distribution of discrete nonlinearities for large η, a positive constant defined below.

Case 1. There is a sequence of points on the real line, x_k, $k=1,\ldots,N$, with N finite or infinite, where the function β reaches a maximum

$$\beta(x)=\sum_{k=1}^{N} e^{-\eta(x-x_k)^2}. \qquad (3)$$

Case 2. There is a sequence of lines in the plane, y_k, $k=1,\ldots,N$, with N finite or infinite, where the function β, independent of x, reaches a maximum

*Electronic mail: horacio@cs.brandeis.edu

$$\beta(x,y)=\sum_{k=1}^{N} e^{-\eta(y-y_k)^2}. \tag{4}$$

Case 3. There is a sequence of points in the plane, (x_k,y_j), $k=1,\ldots,N$, $j=1,\ldots,M$ with N and M finite or infinite, where the function β reaches a maximum

$$\beta(x,y)=\sum_{k=1}^{N}\sum_{j=1}^{M}\sigma(x-x_k,y-y_j;\eta),$$
$$\text{where}\quad \sigma(x,y;\eta)=e^{-\eta(x^2+y^2)}. \tag{5}$$

Case 4. There is a sequence of circles in the plane, $\rho=\rho_k$, $k=1,\ldots,N$, with N finite or infinite, and where ρ represents the radial polar coordinate, where the function β reaches a maximum

$$\beta(\rho)=\sum_{k=1}^{N} e^{-\eta(\rho-\rho_k)^2}. \tag{6}$$

We refer to the points x_k and (x_k,y_j), $k=1,\ldots,N$, and $j=1,\ldots,M$ as quasidiscrete (QD) sites and to the stripes $y=y_k$ and circles $\rho=\rho_k$, $k=1,\ldots,N$ as quasi-semidiscrete (QS) sites. We define d to be the minimum distance between two adjacent QD or QS sites. Note that the function β can be chosen to depend not only on the spatial variable but also on t. The specific form of $\beta(x,y,t)$ will depend on the particular model. One might, for example, have the product of a spatially dependent function $\beta(x,y)$ with a probabilistic time-dependent function.

For Eq. (2) we define the following dimensionless variables and parameters:

$$\hat{x}=\frac{x}{d},\quad \hat{y}=\frac{y}{d},\quad \hat{t}=\frac{\sqrt{D}t}{d} \tag{7}$$

and

$$\epsilon=\sqrt{\frac{D}{\alpha}}\frac{1}{d},\quad \hat{\gamma}=\frac{\gamma d}{\sqrt{D}},\quad \hat{\eta}=\eta d^2,\quad \hat{h}=\frac{h}{\epsilon}. \tag{8}$$

Substituting Eqs. (7) and (8) into Eq. (2) and dropping the $\hat{}$ from the variables and parameters we obtain

$$\epsilon^2\phi_{tt}+\epsilon^2\gamma\phi_t=\epsilon^2\Delta\phi+\beta(x,y)[f(\phi)+\epsilon h]. \tag{9}$$

We will consider the case $0<\epsilon\ll 1$, i.e., when diffusion is slow, d is large or α is large, and there is a small dissipation.

The homogeneous version of Eq. (9)

$$\epsilon^2\phi_{tt}+\epsilon^2\gamma\phi_t=\epsilon^2\Delta\phi+f(\phi)+\epsilon h, \tag{10}$$

possesses a traveling kink solution. The point on the line (for $n=1$) or the set of points in the plane (for $n=2$) for which the order parameter ϕ vanishes are called the interface or front of the system. For Eq. (10) the front moves according to an extended version of the Born-Infeld equation [19,20]

$$(1-s_t^2)s_{xx}+2s_xs_ts_{xt}-(1+s_x^2)s_{tt}-\gamma s_t(1+s_x^2-s_t^2)$$
$$-\hat{h}(1+s_x^2-s_t^2)^{3/2}=0, \tag{11}$$

where $y=s(x,t)$ is the Cartesian description of the interface, and $\hat{h}$, proportional to h, will be defined later. Planar fronts moving according to Eq. (11) with $\gamma=\hat{h}=0$ (no dissipation and both phases with equal potential) move with a constant velocity equal to their initial velocity. For other values of γ or $\hat{h}$, fronts move with a velocity that asymptotically approaches $-\hat{h}/(\gamma^2+\hat{h}^2)^{1/2}$ as long as the initial velocity is bounded from above by 1 in absolute value. Linear perturbations to these planar fronts decay, either in a monotonic or an oscillatory way, to zero as $t\to\infty$ [20]. Circular interfaces moving according to Eq. (11) with $h>0$ shrink to a point in finite time [19,20]. If $h<0$, then circles shrink to points for some initial conditions and for others they grow unboundedly. Neu [19] showed that for $\gamma=h=0$, closed kinks can be stabilized against collapse by the appearance of short-wavelength, small amplitude waves. For the more general case, two situations are possible. Either linear perturbations to a circle decay and curves shrink to a point in finite time or they are still present at the shrinkage point of the circle. Note that Eq. (11), expressed in terms of its kinematic and geometric properties, reads [20]

$$\frac{dv}{dt}+\gamma v(1-v^2)-\kappa(1-v^2)+\hat{h}(1-v^2)^{3/2}=0, \tag{12}$$

where κ is the curvature of the front and dv/dt is the ''Lagrangian'' time derivative of v, which is calculated along the trajectory of the interfacial point moving with the normal velocity v [20].

One of the goals of this paper is to determine whether the dynamic behavior of kinks in Eq. (9) differs from its homogeneous (discrete) nonlinearity counterpart Eq. (10). For the overdamped version of Eq. (2), which is a parabolic bistable equation, it has been shown that there are essential differences between the homogeneous and nonhomogeneous (discrete) cases, in that the latter exhibits propagation failure [8,10,17,18,21].

In Sec. II we present an equation of motion for the front of Eq. (9), and we briefly describe the method by which it was derived. This equation generalizes Eq. (11) with the strong nonlinearity accounting for the influence of the function β on the front motion. In Sec. III we study the evolution of one-dimensional fronts. We show that for $h=0$ the function β acts as a ''potential function'' for the motion of the front, i.e., a front initially placed between two maxima of β asymptotically approaches the intervening minimum. When $h\neq 0$, fronts that start between two maxima of β asymptotically approach an equilibrium point determined by h and β, producing a kink propagation failure. In Sec. IV we study the evolution of two-dimensional fronts with radial symmetry. We find that when there is no dissipation circles can shrink to a point in finite time, grow unboundedly, or their radius can oscillate, depending on the initial conditions. When dissipation effects are present, the oscillations decay spirally or not, depending on the value of γ. The final result is the

stabilization of a circular domain of one phase inside the other phase. Our conclusions appear in Sec. V.

II. FRONT DYNAMICS: THE EQUATION OF MOTION

For Eq. (9) the law of motion of the interface in two dimensions is given by

$$(1-s_t^2)s_{xx}+2s_xs_ts_{xt}-(1+s_x^2)s_{tt}-\gamma s_t(1+s_x^2-s_t^2) - \frac{\beta_y(x,s)-\beta_x(x,s)s_x+\beta_t(x,s)s_t}{2\beta(x,s)}(1+s_x^2-s_t^2) - \hat{h}\beta^{1/2}(x,s)(1+s_x^2-s_t^2)^{3/2}=0, \tag{13}$$

where $\hat{h}$ is proportional to h as will be explained later. Equation (13) was obtained by carrying out a nonrigorous but self-consistent singular perturbation analysis for $\epsilon \ll 1$, treating the interface as a moving internal layer of width $O(\epsilon)$. We focused on the dynamics of the fully developed layer, and not on the process by which it was generated. The method that we applied is similar to that used in Refs. [20] and [21] for the study of the evolution of kinks in both the nonlinear wave equation (10) and the Allen-Cahn equation with quasidiscrete sources of reaction [the overdamped version of Eq. (2)]. The following basic assumptions were made:

(1) For small $\epsilon \geqslant 0$ and all $t \in [0,T]$, the domain Ω can be divided into two open regions: $\Omega_+(t;\epsilon)$ and $\Omega_-(t,\epsilon)$ by a curve $\Gamma(t;\epsilon)$, which does not intersect $\partial\Omega$. This interface, defined by $\Gamma(t;\epsilon) := \{x \in \Omega : \phi(x,t;\epsilon)=0\}$, is assumed to be smooth, which implies that its curvature and its velocity are bounded independently of ϵ.

(2) There exists a solution $\phi(x,t;\epsilon)$ of Eq. (2), defined for small ϵ, for all $x \in \Omega$ and for all $t \in [0,T]$ with an internal layer. As $\epsilon \to 0$ this solution is assumed to vary continuously through the interface, taking the value 1 when $x \in \Omega_+(t;\epsilon)$, -1 when $x \in \Omega_-(t,\epsilon)$, and varying rapidly but smoothly through the interface.

(3) The curvature of the front is small compared to its width.

As a first stage in the derivation of Eq. (13) we define, near the interface, a new variable $z=(y-s)/\epsilon$, which is $\mathcal{O}(1)$ as $\epsilon \to \infty$ and then express Eq. (9) in terms of this new variable. Next we expand ϕ and β asymptotically in power series in ϵ and substitute these expansions into the differential equation. After equating the coefficients of corresponding powers of ϵ, we obtain two equations. The first can be reduced to an equation of the type $\Phi^0_{zz}+f(\Phi^0)=0$, which has to satisfy $\Phi^0(0)=0$ and $\Phi^0(\pm 1)=\pm 1$, giving a kink solution. Here Φ^0 represents the leading-order term of the order parameter ϕ in terms of z. The second problem is a linear nonhomogeneous second- order ODE. Equation (13) is obtained by applying the solvability condition (Fredholm alternative) after defining $\hat{h} := h[\Phi^0(+\infty)-\Phi^0(-\infty)]/\int_{-\infty}^{\infty}(\Phi^0_z)^2 dz$. Note that for $f(\phi)=(\phi-\phi^3)/2$ (Ginsburg-Landau theory), $\Phi^0(z)=\tanh(z/2)$ and $\hat{h}=3h$, whereas for $f(\phi)=\sin\phi$ (sine-Gordon), $\Phi^0(z)=4\tan^{-1}e^z-\pi$ and $\hat{h}=(\pi/4)h$.

III. FRONT MOTION IN ONE DIMENSION

For a one-dimensional system, Eq. (13) reads

$$s_{tt}+\gamma s_t(1-s_t^2)+\frac{\beta'(s)}{2\beta(s)}(1-s_t^2)+\hat{h}\beta^{1/2}(s)(1-s_t^2)^{3/2}=0. \tag{14}$$

We concentrate on functions β of the form (3), although the same analysis can be done for a general differentiable function. We define $u=s$ and $v=s_t$ obtaining

$$\begin{cases} u_t = v \\ v_t = -\gamma v(1-v^2)-\dfrac{\beta'(u)}{2\beta(u)}(1-v^2)-\hat{h}\beta^{1/2}(u)(1-v^2)^{3/2}. \end{cases} \tag{15}$$

The fixed points of Eq. (15) are $(u_0,0)$, where u_0 satisfies $g(u)=\beta'(u)+2\hat{h}\beta^{3/2}(u)=0$. The trace τ and determinant Δ of the matrix of the linearized system are $\tau=-\gamma$ and $\Delta=[\beta''(u_0)\beta(u_0)-\beta'^2(u_0)]/2\beta^2(u_0)+\hat{h}\beta'(u_0)/[2\beta^{1/2}(u_0)]$, respectively. If $\hat{h}=0$ then the fixed points are the maxima (unstable) and minima (stable) of $\beta(u)$. Thus, a front initially between two maxima of β, will move and asymptotically approach the intervening minimum. When there is no dissipation, this behavior is in contrast with the homogeneous case (11), where, as was pointed out in the Introduction, fronts move with a constant velocity equal to their initial velocity. In the inhomogeneous case, we can predict the final position of the front from the structure of β. In order to understand the behavior of $g(u)$ as $\hat{h}$ increases above zero we consider a function $\beta(u)$ with a single peak at 0, i.e., $\beta(u)=e^{-\eta u^2}$. This function will approximate the more general Eq. (3) if $\eta \gg 1$, so that the influence of peaks on one another is very small. In this case $g(u)=-2e^{-\eta u^2}[\eta u-\hat{h}e^{-(\eta u^2)/2}]$. For $\hat{h}=0$, $g(u)$ vanishes at $u=0$ and it is positive for $u<0$ and negative for $u>0$. As $\hat{h}$ moves away from zero, $\hat{u}$, the root of $g(u)$, will be given by the solution of $\eta u-\hat{h}e^{-(\eta u^2)/2}=0$, an equation that always has a solution. If $\hat{h}>0$, then $\hat{x}>0$, and $g(u)$ is positive for $x>\hat{x}$ and negative for $x<\hat{x}$. If $\hat{h}<0$, then $\hat{x}<0$. As an illustration, we can see the shape of $g(u)$ as $\hat{h}$ increases in Fig. 1. In summary, as $\hat{h}$ increases or decreases, the behavior of the front is similar to the case $\hat{h}=0$, in contrast to the classical homogeneous case (11) where, as noted in Sec. I, fronts with an initial velocity whose absolute value is bounded from above by 1, move with a velocity that asymptotically approaches $-\hat{h}/(\gamma^2+\hat{h}^2)^{1/2}$.

IV. FRONT MOTION IN TWO DIMENSIONS

The analysis of front motion in two dimensions governed by Eq. (13) with a function β of type (4), reduces to the analysis of one-dimensional front motion, and we shall not consider this case further. For radially symmetric functions, $\beta=\beta(\rho)$, and radially symmetric fronts, Eq. (13) for the radial coordinate ρ of the front reads

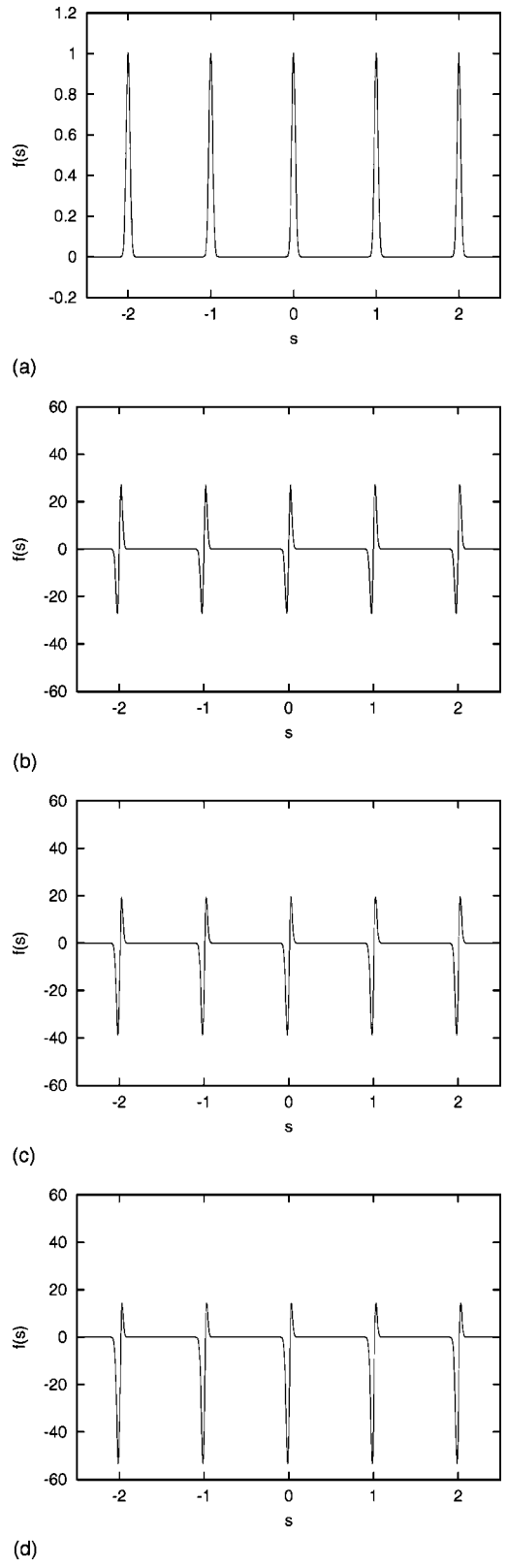

FIG. 1. (a) Graph of $\beta(u)$ for $\eta=1000$, $x_1=2$, $x_2=1$, $x_3=0$, and $x_4=-1$, $x_5=-2$. (b) Graph of $g(u)$ for $\eta=1000$, $h=0$, $x_1=2$, $x_2=1$, $x_3=0$, and $x_4=-1$, $x_5=-2$. (c) Graph of $g(u)$ for $\eta=1000$, $h=10$, $x_1=2$, $x_2=1$, $x_3=0$, and $x_4=-1$, $x_5=-2$. (d) Graph of $g(u)$ for $\eta=1000$, $h=20$, $x_1=2$, $x_2=1$, $x_3=0$, and $x_4=-1$, $x_5=-2$. The points x_k are the maxima of $\beta(u)$.

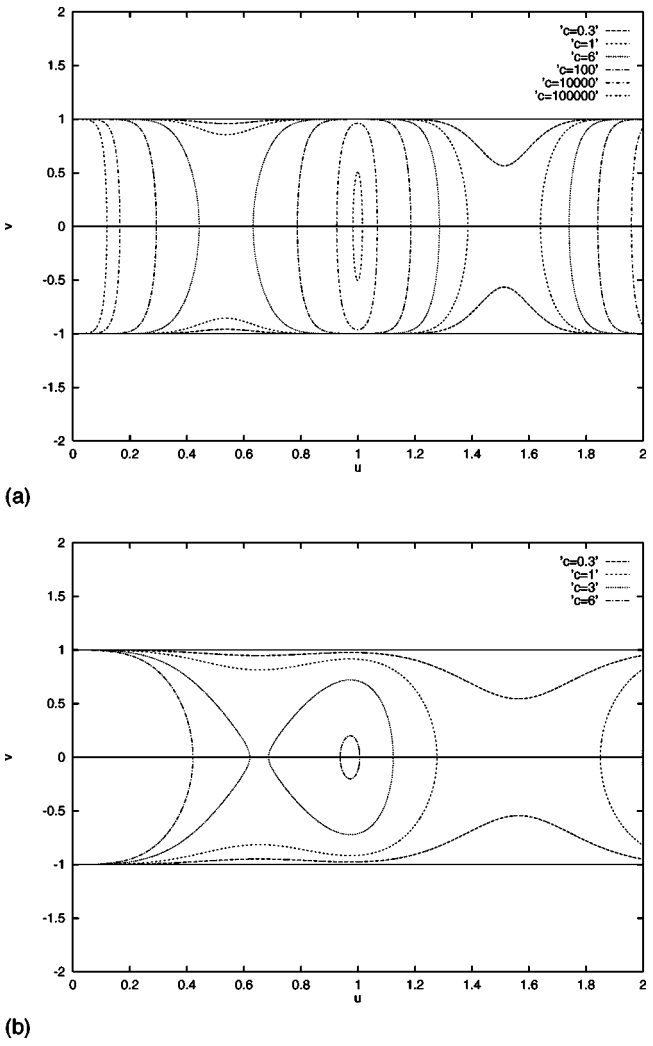

FIG. 2. Graph of Eq. (18) with β given by Eq. (4) with $N=2$, $\rho_1=0.5$, $\rho_2=1.5$, and (a) $\eta=50$; (b) $\eta=10$.

$$\rho_{tt}+\left(\gamma\rho_t+\frac{1}{\rho}\right)(1-\rho_t^2)+\frac{\beta'(\rho)}{2\beta(\rho)}(1-\rho_t^2)+\beta^{1/2}(\rho)\hat{h}(1-\rho_t^2)^{3/2}. \tag{16}$$

We define $u=\rho$ and $v=\rho_t$ obtaining

$$\begin{cases} u_t=v \\ v_t=-\left[\gamma v+\dfrac{1}{u}+\dfrac{\beta'(u)}{2\beta(u)}+\hat{h}\beta^{1/2}(u)(1-v^2)^{1/2}\right](1-v^2). \end{cases} \tag{17}$$

The lines $v=\pm 1$ are trajectories of Eq. (17) in the corresponding phase plane. They define a region D with the property that every curve starting in this region remains inside it for all future time. Here we analyze the case $\hat{h}=0$ and confine our analysis to $u>0$. The fixed points of Eq. (17) are $(u_0,0)$, where u_0 are solutions (if they exist) of $2\beta(u)+u\beta'(u)=0$. The trace τ and the determinant Δ of the matrix of the linearized system are given by $\tau=-\gamma$ and $\Delta=-1/u_o^2+[\beta''(u_0)\beta(u_0)-\beta'^2(u_0)]/2\beta^2(u_0)$, respectively.

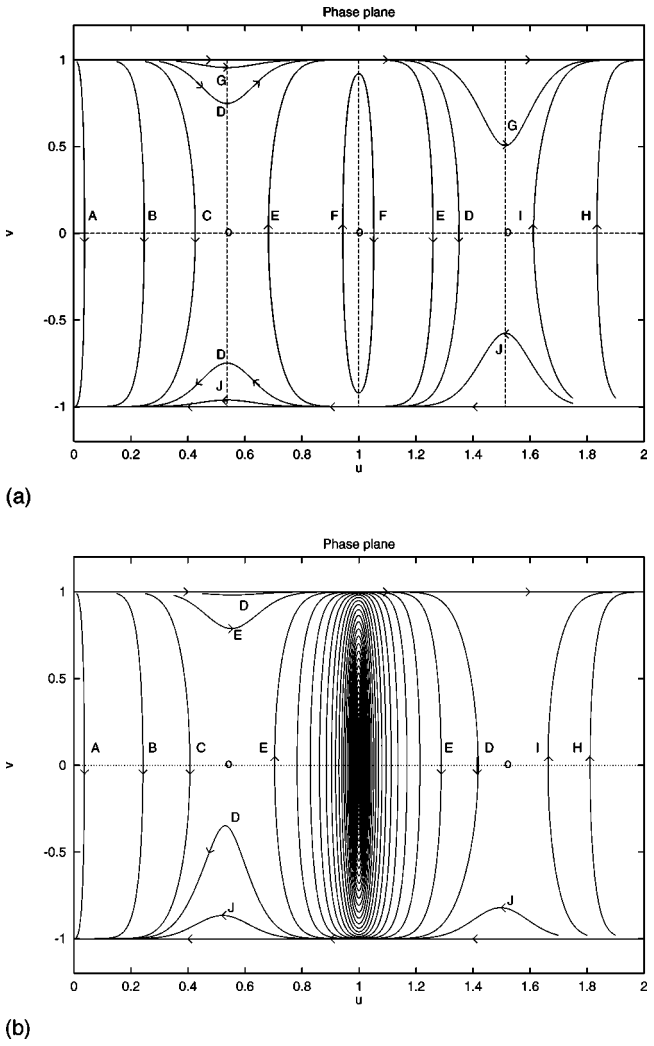

FIG. 3. Phase plane for Eq. (17) with β given by Eq. (4) with $N=2$, $\rho_1=0.5$, $\rho_2=1.5$, $\eta=50$, and $\hat{h}=0$. The dashed lines are the nullclines of the system and the o are its fixed points. (a) $\gamma=0$; (b) $\gamma=1$.

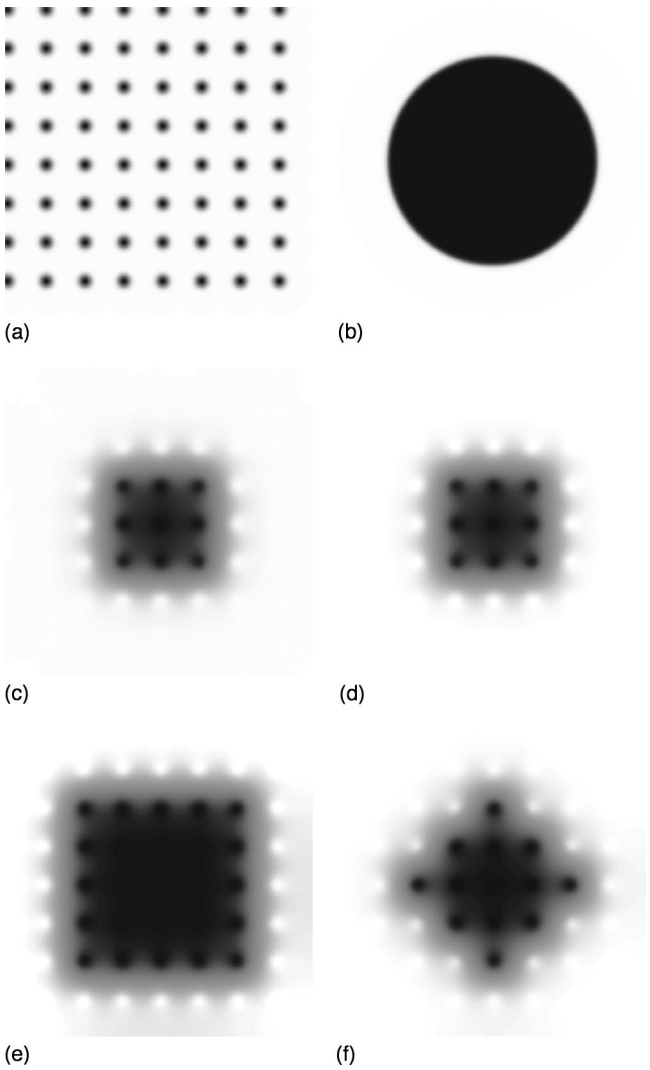

FIG. 4. (a) Graph of $\beta(x,y)$ given by Eq. (5) with $\eta=50$. In the gray scale, white corresponds to $\beta=0$ and black corresponds to $\beta=1$. The distance between neighboring maxima along the x or y axes is 1. (b) Circle of radius 2.0 embedded in the net given in (a). The black part corresponds to $\phi=+1$ and the white part corresponds to $\phi=-1$. It serves as the initial condition for Eq. (9). (c) Steady state for the evolution of the initial condition given in (b) according to Eq. (9) with $\epsilon=0.1$, $\gamma=1$, $h=0$, and β given as in (a). (d) Steady state for the evolution of the initial condition given in (b) according to Eq. (9) with $\epsilon=0.1$, $\gamma=5$, $h=0$, and β given as in (a). (e) Steady state for the evolution of the initial condition given in (b) according to Eq. (9) with $\epsilon=0.1$, $\gamma=1$, $h=1$, and β given as in (a). (f) Steady state for the evolution of the initial condition given in (b) according to Eq. (9) with $\epsilon=0.1$, $\gamma=5$, $h=1$, and β given as in (a).

The simplest case is $\beta(\rho)=e^{-\eta(\rho-\rho_1)^2}$ for a given $\rho_1>0$ $(N=1)$. For this case $u_0=(\eta\rho_1+\sqrt{\eta^2\rho_1^2+4\eta})/2\eta$ and $(u_0,0)$ is a saddle point. For $N>2$, assume that $g(u)=2\beta(u)+u\beta'(u)$ has $2N-1$ isolated roots $u_1,u_2,\ldots,u_{2N-1}$ and that $g'(u_{2k-1})<0$ and $g'(u_{2k}>0)$, $k=1,\ldots,N$. For the case $\gamma=0$, dividing the second equation in Eq. (17) by the first and solving, one obtains

$$c^2u^2\beta(u)+v^2=1, \tag{18}$$

where $c^2=(1-v_i^2)/u_i^2\beta(u_i)$ and (u_i,v_i) are the initial conditions. We can define an ''energy'' function $E=(1-v^2)/u^2\beta(u)$. It can be shown that E is constant on trajectories of Eq. (17) and that u_{2k}, $k=1,\ldots,N$ are local minima of E. Then all trajectories sufficiently close to u_{2k} are closed, and u_{2k} are nonlinear centers [22]. This means that when there is no dissipation the radii of circular interfaces close enough to u_{2k} oscillate arround u_{2k}. For Eq. (4) with $\eta=50$ and $N=2$, $\rho_1=0.5$ and $\rho_2=1.5$, we calculated the fixed points of Eq. (17) using the Newton-Raphson method with a tolerance of 0.0001. They are $z_1=0.537\,228$, $z_2=0.999\,165$, and $z_3=1.513\,217$. The corresponding values of Δ are $\Delta(z_1)=-53.464\,832$, $\Delta(z_2)=1196.824\,463$, and $\Delta(z_3)=-50.436\,714$. Then z_1 and z_3 are saddle points, and z_2 is stable. Since the discriminant, $\Lambda=\tau^2-4\Delta$ of z_2, is $-4787.297\,852<0$, z_2 is a neutrally stable center for $\gamma=0$, a stable spiral for $0<\gamma\leqslant\gamma_0$, and a stable node for $\gamma>\gamma_0$,

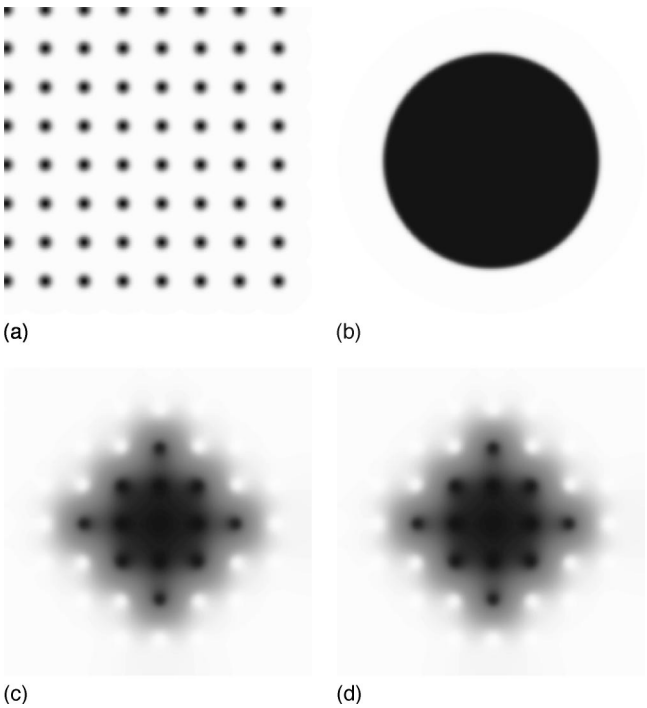

FIG. 5. (a) Graph of $\beta(x,y)$ given by Eq. (5) with $\eta=50$. In the color scale, white corresponds to $\beta=0$ and black corresponds to $\beta=1$. The distance between neighboring maxima along the x or y axes is 1. (b) Circle of radius 2.2 embedded in the net given in (a). The black part corresponds to $\phi=+1$ and the white part corresponds to $\phi=-1$. It serves as the initial condition for Eq. (9). (c) Steady state for the evolution of the initial condition given in (b) according to Eq. (9) with $\epsilon=0.1$, $\gamma=1$, $h=0$, and β given as in (a). (d) Steady state for the evolution of the initial condition given in (b) according to Eq. (9) with $\epsilon=0.1$, $\gamma=5$, $h=0$, and β given as in (a).

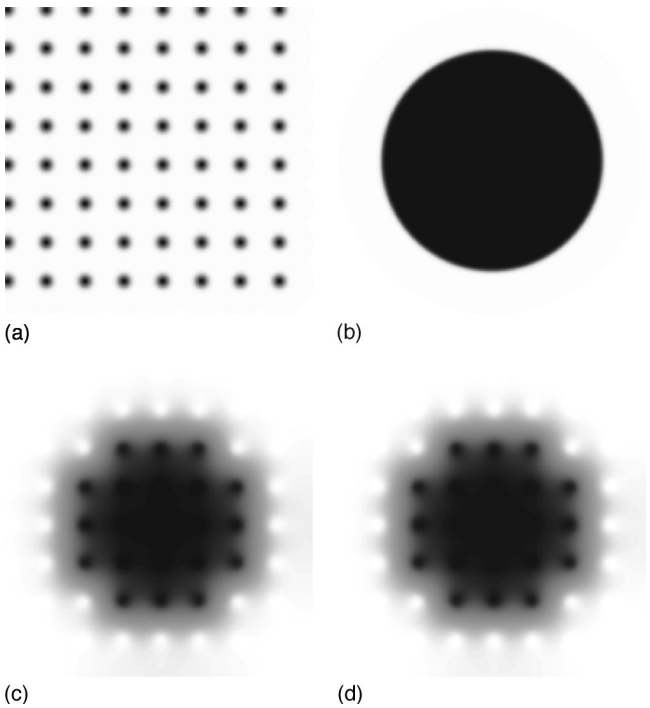

FIG. 6. (a) Graph of $\beta(x,y)$ given by Eq. (5) with $\eta=50$. The color scale goes from white $\beta=0$ to black $\beta=1$. (b) Circle of radius 2.4 embedded in the net given in (a). The black part corresponds to $\phi=+1$ and the white part corresponds to $\phi=-1$. It serves as the initial condition for Eq. (9). (c) Steady state for the evolution of the initial condition given in (b) according to Eq. (9) with $\epsilon=0.1$, $\gamma=1$, $h=0$, and β given as in (a). (d) Steady state for the evolution of the initial condition given in (b) according to Eq. (9) with $\epsilon=0.1$, $\gamma=5$, $h=0$, and β given as in (a).

where γ_0 is the value of γ for which $\Lambda=0$. In Fig. 2 we present a graph of Eq. (18) for β given by Eq. (4) with $N=2$, $\rho_1=0.5$, $\rho_2=1.5$, $\eta=50$ (a), and $\eta=10$ (b). We observe that there are shrinking trajectories, oscillatory trajectories, and growing trajectories, in contrast with the homogeneous case where all trajectories are shrinking trajectories given by $c^2u^2+v^2=1$ with $c^2=(1-v_i^2)/u_i^2$ [20]. As η decreases, the oscillatory trajectories dissappear, leaving growing trajectories, which will ultimately vanish as $\eta\to 0$.

In order to study more generally the behavior of the system away from the fixed points, we present in Fig. 3 the phase plane for $\gamma=0$ (a) and $\gamma=1$ (b). The dashed lines are the nullclines of the system and the ''o'' are its fixed points. The trajectories were calculated by solving Eq. (17) using a Runge-Kutta method of order four. We observe there that there are different situations according to the initial conditions. In Fig. 3(a) (no dissipation), trajectories *A*, *B*, and *C* correspond to circles that shrink to a point in finite time. If their initial velocity is positive, then their radius grows initially to a value bounded by z_1 before shrinkage takes place. Trajectories *D* and *J* also correspond to a circles that finally shrink to a point in finite time. In the case of *D*, although the initial conditions are close to those of trajectory *C*, the dynamics are very different. In addition to shrinkage, trajectories can display unbounded growth, represented by trajectory *G*, and periodic behavior, represented by trajectories *E* and *F*. Trajectories *H* and *I* also correspond to circles growing unboundedly, but if the initial velocity is negative they shrink to a valued bounded from below by z_3 and then they start growing. In Fig. 3(b) ($\gamma=1$) we see that trajectories *A*, *B*, and *C* correspond to circles that shrink to points in finite time after growing to a radius bounded by z_1. Trajectory *D* also shrinks to a point in finite time, but it grows initially to a radius bounded from above by z_3 and from below by z_2. As we pointed out before, as a consequence of dissipation ($\gamma\neq 0$), z_2 is a stable spiral. We see that trajectory *E* spirals into z_2, and there are no longer periodic trajectories. For $N>2$ we expect the phase plane analysis to be similar to that presented here. In contrast with the homogeneous nonlinear wave equation, where any circular front shrinks to a point in finite time, the nonhomogeneous version (13) presents a very rich dynamics with periodic motion and stabilization of circular domains of one phase inside the other.

In the absence of dissipation there are two ''forces'' responsible for the motion of the front; the curvature of the circular front $1/\rho$ and the ''potential function'' β. For initial conditions near enough to the minimum of β, the two ''forces'' balance giving arise to nonlinear centers (or spiral nodes). Oscillations are possible due to the term $1-v^2$.

When dissipation is present the ''balance'' is still present but the oscillations decay.

In order to study more general cases than the radially symmetric we have performed numerical simulations of the original two-dimensional model (9) with $\epsilon=0.1$, with the amplitude $\beta(x,y)$ given by Eq. (5). We have used a split-step semi-implicit time integration method. The gray-scale portraits of the results are presented in Figs. 4–6. The figures are organized as follows. As a first picture (a), each figure contains two-dimensional (2D) plot of $\beta(x,y)$. The distance between neighboring sites of $\beta(x,y)$ is always 1, black and white in the gray scale correspond to a maximum (1) and a minimum (0) of β, respectively. Then (b) follows, an initial circular configuration of $\phi(x,y)$ used for the particular simulations. Black and white in the gray scale correspond to $\phi=+1$ and $\phi=-1$, respectively. The circle is centered at a maximum of β. Finally, there are several final configurations of $\phi(x,y)$, to which simulations with different sets of parameters have converged after a long enough run. In particular, Fig. 4 illustrates a series of simulations with the initial circle of radius $r_0=2.0$. This radius is chosen, so that the boundary of the domain $\phi=+1$ contains several maxima of $\beta(x,y)$. This choice makes the initial configuration especially unstable and capable of nontrivial subsequent evolution. Indeed, as we see from Figs. 4 (c)–4(f), that evolution is sensitive to the parameters of the simulations, such as asymmetry in the potential h and dissipation γ. Figures 5 and 6 represent results obtained for an initial radius close to the one in Fig. 4 ($r_0=2.2$), and farther from it ($r_0=2.4$). In the former case [Figs. 5(c) and 5(d)] the evolution converges to a steady state of a size close to the one obtained for $r_0=2.0$ [compare to Figs. 4(c) and 4(d)], while in the latter case [Figs. 6(c) and 6(d)] the size of the resulting steady state is different.

V. CONCLUSIONS

In this paper we have presented Eq. (13) as governing the evolution of a fully developed front in a inhomogeneous version of the nonlinear wave equation, Eq. (9), when $\epsilon \ll 1$. This equation generalizes the damped version of the Born-Infeld equation (11) to include the effects of stronger nonlinearities and accounts for the influence of the nonhomogeneous nonlinear term on the motion of the front. The motion of interfaces according to Eq. (13) is qualitatively different from that of the homogeneous counterpart given by Eq. (11). This difference arises primarily from the fact that the function β acts as a potential function for the motion of the front. For the one-dimensional case, an initial front initially placed between two maxima of β which for a homogeneous nonlinear term will move with a velocity that asymptotically approaches $-\hat{h}/(\gamma^2+\hat{h}^2)^{1/2}$ as long as the initial velocity, bounded from above by 1 in absolute value, asymptotically approaches a point depending on $\hat{h}$ and on the structure of β. For the radially symmetric two-dimensional case, the dynamics are richer than in the homogeneous counterpart, where for $\hat{h}=0$ circles shrink to point in finite time. In the absence of dissipation, circles can shrink to a point in finite time, grow unboundedly, or their radius oscillates, depending on the initial conditions. When dissipation effects are present, the oscillations decay, spirally or not, depending on the value of γ. The final result is the stabilization of a circular domain of one phase inside the other phase.

The evolution of circular interfaces in more complicated arrangements of QD sites and the evolution of more complicated fronts, such as convex closed curves, calls for further research. We hope to address these questions in a forthcoming paper.

ACKNOWLEDGMENTS

This work was supported by the financial support of Fischbach to H. G. Rotstein and by the Chemistry Division of the National Science Foundation.

[1] S. Flach and K. Kladko, Phys. Rev. E **54**, 2912 (1996).
[2] S. Flach and C.R. Willis, Phys. Rep. **295**, 181 (1998).
[3] L.M. Floria and J.J. Mazo, Adv. Phys. **45**, 505 (1996).
[4] H. Fukuyama and P.A. Lee, Phys. Rev. B **17**, 535 (1978).
[5] P.A. Lee and T.M. Rice, Phys. Rev. B **19**, 3970 (1979).
[6] S.N. Coppersmith, Phys. Rev. Lett. **65**, 1044 (1990).
[7] A.R. Bishop, B. Horovitz, and P.S. Lomdahl, Phys. Rev. B **38**, 4853 (1988).
[8] I. Mitkov, K. Kladko, and J.E. Pearson, Phys. Rev. Lett. **81**, 5453 (1998).
[9] I. Mitkov, K. Kladko, and A.R. Bishop, Phys. Rev. E **61**, 1106 (2000).
[10] I. Mitkov, Physica D **133**, 398 (1999).
[11] K. Kladko, I. Mitkov, and A. R. Bishop, Phys. Rev. Lett. **84**, 4505 (2000).
[12] S. Ponce Dawson, J. Keizer, and J.E. Pearson, Proc. Natl. Acad. Sci. U.S.A. **96**, 6060 (1999).
[13] J. Keizer, G.D. Smith, S. Ponce Dawson, and J.E. Pearson, Biophys. J. **75**, 595 (1998).
[14] J.E. Pearson and S. Ponce Dawson, Physica A **257**, 141 (1998).
[15] G. Gruner, Rev. Mod. Phys. **60**, 1129 (1988).
[16] G. Gruner, Rev. Mod. Phys. **66**, 1 (1994).
[17] J.P. Keener, Physica D **136**, 1 (2000).
[18] J. P. Keener, Siam J. Appl. Math. **61**(1), 317 (2000).
[19] J.C. Neu, Physica D **43**, 421 (1990).
[20] H.G. Rotstein and A.A. Nepomnyashchy, Physica D **136**, 245 (2000).
[21] H. G. Rotstein, A. M. Zhabotinsky, and I. R. Epstein (unpublished), http://xxx.lanl.gov, e-print nlin.PS/0002042
[22] S. H. Strogatz, *Nonlinear Dynamics and Chaos* (Addison-Wesley, Reading, MA, 1997).